Laser nanostructuring of polymers: Ripples and applications

Marta Castillejo, Tiberio A. Ezquerra, Margarita Martín, Mohamed Oujja, Susana Pérez et al.

Citation: AIP Conf. Proc. **1464**, 372 (2012); doi: 10.1063/1.4739891
View online: http://dx.doi.org/10.1063/1.4739891
View Table of Contents: http://proceedings.aip.org/dbt/dbt.jsp?KEY=APCPCS&Volume=1464&Issue=1
Published by the AIP Publishing LLC.

Laser Nanostructuring of Polymers: Ripples and Applications

Marta Castillejo[a,*], Tiberio A. Ezquerra[b], Margarita Martín[a], Mohamed Oujja[a], Susana Pérez[a], Esther Rebollar[a]

[a] *Instituto de Química Física Rocasolano, CSIC, Serrano 119, 28006 Madrid, Spain*

[b] *Instituto de Estructura de la Materia, CSIC, Serrano 121, 28006 Madrid, Spain*

**Email: marta.castillejo@iqfr.csic.es*

Abstract. Polymer nanostructures and nanopatterns are being profusely used for developing next-generation organic devices with analytical and biological functions and photonic applications. Laser based strategies constitute an advantageous approach for the assembly and control of this type of soft matter nanostructures as they afford the sought versatility and reliability. Recent and on-going research on laser nanostructuring of thin films of synthetic polymers and natural biopolymers will be exemplified by studies on the generation of laser induced periodic surface structures (LIPSS) and their use for surface enhanced Raman spectroscopy (SERS) based sensors.

Keywords: Laser nanoprocessing, Laser induced periodic surface structuring, soft matter, polymers, biopolymers, SERS
PACS: 42.62.-b, 68.35.bm

INTRODUCTION

Small length scale structuring of polymeric materials provides a variety of substrates to be used in many fields straddling from organic photonics and micro electronics to biomedicine [1-9]. In the last few years, soft lithography methods, such as micro-contact printing or nanoimprint lithography, have been developed for the micro and nanoprocessing of polymer materials aiming at simplicity, reproducibility and low-cost [1]. However when dealing with biomaterials some of these methods are prone with difficulties due to their typical non biocompatibility. Alternative approaches are searched for and in particular laser-based methods are good candidate tools in high-resolution patterning of polymeric materials as they afford the sought versatility and reliability [2-9].

Strongly absorbed UV laser pulses with durations ranging from nanoseconds (ns) to femtoseconds (fs) have been used for the generation of superficial nanostructures in biopolymer films. In [10] it was shown that laser irradiation of thin films of chitosan, starch and their blend with 500 fs pulses of 248 nm resulted in the formation of a layer in the form of interconnected pores and bubbles. However when longer picosecond (ps) and ns pulses were applied, this effect developed only in chitosan. The differences were explained on the basis of the mechanisms operating under the different pulse

International Symposium on High Power Laser Ablation 2012
AIP Conf. Proc. 1464, 372-380 (2012); doi: 10.1063/1.4739891

temporal domains and of the material properties, particularly extinction coefficient and thermal parameters, which determine the amplitude of the laser-induced pressure wave. Successful cell culture on the laser induced foamed chitosan was demonstrated proving the broad potential of laser generated 2D and 3D structures in biological applications.

For some applications, especially in photonics and sensing, generation of periodic nanostructures in polymeric materials offers an array of novel opportunities [11]. Laser induced periodic surface structures (LIPSS) have been generated on polymeric substrates at fluences below the ablation threshold at various wavelengths under ns and fs irradiation regimes in several synthetic polymers [6,7,12-15]. The period of the ripples is of the order of the laser wavelength and their formation has been explained on the basis of the interference between the incident laser light wave and surface-scattered waves created during irradiation [16].

The present contribution gives account of investigations of LIPSS on several polymeric substrates aiming at control and tunability of the size and morphology of the periodic structures while ensuring photochemical integrity of the polymer material. We report on the generation of LIPSS with periods similar to the irradiation wavelength and parallel to the laser polarization direction on thin films of poly (ethylene terephthalate), poly (trimethylene terephthalate) and poly (carbonate bisphenol A) using linearly polarized pulses from a Q-switched Nd:YAG laser (6 ns at 266 nm) and a Ti:sapphire laser (120 fs at 795 nm and 260 fs at 265 nm). LIPSS formation has been also investigated on self-standing films of the biopolymer chitosan and of its blend with the polymer polyvinylpyrrolidone in the ns domain using an ArF excimer laser (193 nm) and the 4th (266 nm) and 5th (213 nm) harmonics of the Nd:YAG laser. Analysis of the nanostructures is carried out by atomic force microscopy complemented by grazing incidence small angle X-ray scattering (GISAXS) which provides additional structural information [6,17,18]. We also report on the application of polymer LIPSS as substrates for surface enhanced Raman spectroscopy (SERS). To this end the rippled polymer films were coated with a uniform gold layer by pulsed laser deposition. It was found that the LIPSS relief resulted on a substantial enhancement of the Raman signal, measured as a factor of 10-15, for a highly diluted aqueous thiophenol solution.

EXPERIMENTAL

Irradiation of the polymeric substrates was carried out in ambient air with linearly polarized laser light. Several pulsed laser systems were used and their most important characteristics are summarized in Table 1. The synthetic polymer samples were based on poly (ethylene terephthalate) (PET) (Rhodia S80 from RhodiaSter), poly (trimethylene terephthalate) (PTT), polycarbonate bisphenol A (PC) (Lexan ML3021A, SABIC I-P (Innovative Plastics)) and poly (vinylidene fluoride) (PVDF) (Solef 6010, Solvay, Germany). While PET, PTT and PC can be easily obtained in the fully amorphous state at room temperature by fast quenching from the molten state, PVDF is typically semicrystalline. Polymer thin films of about 150 nm thickness were prepared by spin coating on silicon wafers (100), polished on both surfaces. Full details of the preparation procedure are given in [6]. Self standing films of the

biopolymer chitosan (Aldrich) and a 50/50 wt. % blend with the synthetic polymer polyvinylpyrrolidone (PVP) were prepared by the method of solvent evaporation resulting in a final thickness of ca. 180 μm [10]. UV-visible absorption spectra of the different materials casted on quartz substrates were recorded with a UV-visible spectrophotometer (Perkin Elmer U/V Lambda 16) in the range of 190-800 nm. The linear absorption coefficients determined for the different wavelengths employed for irradiation are reported in Table 2.

The topography of the polymer films was examined by atomic force microscopy (AFM, Nanoscope IIIA Multimode, Veeco) in tapping mode and images were analysed with the software Nanoscope Analysis 1.10. The original samples present a flat surface, with mean roughness values ≤ 3 nm. The periods and heights of LIPSS were determined from AFM analysis by averaging the results of three different areas per sample. Values of the period were derived from fast Fourier transform (FFT) analysis. Irradiated areas were also analyzed by grazing incidence small-angle X-ray scattering (GISAXS) using the facilities of the BW4 beamline at HASYLAB (DESY, Hamburg). Details of GISAXS measurements are given in [6].

Finally for the SERS experiments, the nanostructured polymer films were coated with a uniform gold layer by the method of pulsed laser deposition (PLD). A gold target was ablated in a stainless-steel vacuum deposition chamber pumped down to 6 $\times 10^{-5}$ Pa [19] using the 5th harmonic (213 nm) of a Q-switched Nd:YAG laser operating at a repetition rate of 10 Hz. The laser beam was focused by a 25 cm focal length lens to yield fluences up to 2 J/cm^2 and the nanostructured polymer samples were placed at 4 cm in front of the target. Deposits were grown at room temperature by delivering up to 36000 pulses to the target which resulted in a deposition time of up to one hour. The morphology of the coated polymer samples was again characterized by AFM and GISAXS. Raman spectra were recorded with an InVia Raman microscope (Renishaw), equipped with a high sensitivity ultra-low noise CCD and a diode laser with emission at 785 nm as the excitation source, operating at a power level of 5 mW (1% of the total laser power). The spectra were acquired by collecting scattered light in back scattering geometry, using a magnification objective x100. Acquisition time and accumulations were 20 s and 10 respectively. The spectral resolution was 2 cm^{-1}.

TABLE 1. Characteristics of the laser systems used to generate LIPSS in polymeric substrates.

Laser	**Wavelength**	**Pulse duration (full with half maximum)**
ArF excimer	193 nm	15 ns
Nd:YAG (4th harmonic)	266 nm	6 ns
Nd:YAG (5th harmonic)	213 nm	15 ns
Ti:sapphire (3rd harmonic)	265 nm	260 fs
Ti:sapphire	795 nm	120 fs

RESULTS AND DISCUSSION

AFM and GISAX measurements of LIPSS

Figure 1 displays AFM topographic images of LIPSS generated in polymer samples under various laser irradiation conditions. As observed in all cases, the structures have a period close to the laser wavelength and are parallel to the polarization direction of the laser. The range of laser fluences and number of pulses at which generation of well defined LIPSS are observed are listed in Table 2. As indicated, these ranges strongly depend on the material and on the laser wavelength and pulse duration. It is worth noticing that irradiation of PVDF at 266 nm (pulses of 6 ns) does not result in formation of LIPSS. The lack of ripples has been related in this case with the initial polymer crystalline structure or to its weak absorption at the irradiation wavelength [6].

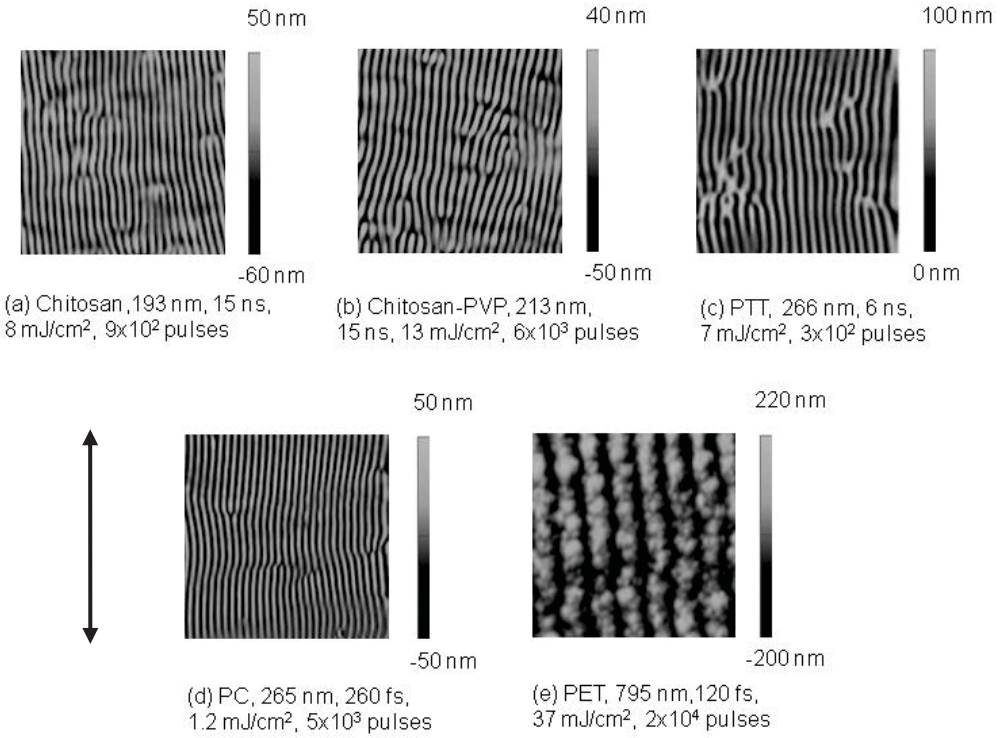

FIGURE 1. AFM height images (5x5 μm^2 size) of LIPSS formed in polymeric substrates under the indicated laser conditions. The double arrow indicates the direction of the laser polarization.

TABLE 2. Linear absorption coefficient and ranges of laser fluence (F) and number of pulses (N) for the generation of well defined LIPSS in polymeric materials under various laser conditions of wavelength and pulse duration.

Material/ laser	α (cm^{-1}) x10^3	F (mJ/cm^2)	N (pulses)
Chitosan/ 193 nm, 15 ns	4.1	12-20	900-1200
Chitosan-PVP/ 193 nm, 15 ns	11.6	10-26	600-1500
Chitosan/ 213 nm, 15 ns	2.0	10-14	3000-8000
Chitosan-PVP/ 213 nm, 15 ns	8.7	9-17	5000-9000
PET/ 266 nm, 6 ns	18	4-10	300-3000
PTT/ 266 nm, 6 ns	26	4-10	100-3000
PC/ 266 nm, 6 ns	18	5-10	800-3000
PVDF/ 266 nm, 6 ns	0.4	-	-
PET/ 265 nm, 260 fs	18	1.0-2.4	500-10000
PTT/ 265 nm, 260 fs	26	1.0-2.4	500-10000
PC/ 265 nm, 260 fs	18	1.0-2.4	500-10000
PET/ 795 nm, 120 fs	0.8	35-40	5000-50000
PTT/ 795 nm, 120 fs	0.7	35-40	5000-50000
PC/ 795 nm, 120 fs	0.4	35-40	5000-50000

The characterization in real space of the nanostructured polymer surfaces by AFM was complemented by characterization in the reciprocal one by GISAXS. Figure 2 shows for laser irradiated PTT sample, under conditions of LIPSS formation, the AFM height image (a) and the corresponding GISAXS pattern (b) characterized by the exit angle, α, and the out of scattering plane angle, ω. The Figure also shows the corresponding intensity profile across the horizontal direction as a function of ω extracted from the GISAXS pattern (at a fixed $\alpha = 0.2^{o}$). Scattering maxima out of the meridian ($\omega \neq 0$) are clearly visible in the range of LIPSS formation. The slight asymmetry observed in the GISAXS pattern is due to the small deviation in the parallelism of the structures along the whole inspected spot. The information provided by GISAXS can be interpreted on the basis of the two orthogonal scattering vectors $q_z = (2\pi/\lambda)\ (\sin\alpha_i + \sin\alpha)$ and $q_y = (2\pi/\lambda)\ \sin\omega\ \cos\alpha$. In these expressions $\lambda = 0.13808$ nm and $\alpha_i = 0.4°$ are the wavelength and incidence angle of the X-ray beam respectively. The scattering vectors provide information about structural correlations perpendicular and parallel to the film plane, respectively. Spacing of the first maximum obtained from the GISAXS pattern can be determined through the expression $L = 2\pi/q_y^{Max}$ where q_y^{Max} is the q-value corresponding to the first intensity maximum, indicated by an arrow in Figure 2(c). Spacing values derived from GISAXS for the irradiated polymers are in very good qualitative correlation with the period determination by AFM.

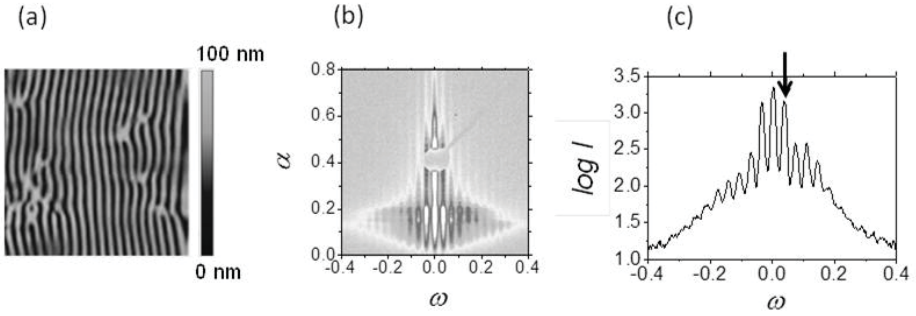

FIGURE 2. (a) AFM height image (5x5 μm^2 size), (b) GISAXS pattern and (c) corresponding cut at $\alpha = 0.2^{\circ}$ of PTT irradiated with 300 pulses at 7 mJ/cm^2. Each point on the GISAXS pattern can be characterized by the exit angle, α, and the out of scattering plane angle, ω, both given in degrees. The arrow in (c) indicates the first intensity maximum.

The wide range of laser conditions explored results in a broad tunability of period dimensions. Also the fact that in all conditions the period of the nanostructures closely follows the irradiation wavelength strongly suggests a common formation mechanism based on the interference between the incident laser light wave and the surface-scattered waves created during irradiation [6,7].

Further control of the period of the structures, L, can be achieved by varying the angle of incidence, θ, of the beam on the surface of the polymer samples. As shown in Figure 3 for a sample of PET, the period of the structures generated by repetitive irradiation with 6 ns pulses at 266 nm can be tuned from about 250 to 500 nm by changing the laser incidence angle from 0 to 45 degrees. Figure 3 also shows the fitting of experimental data to the expected dependence [16]:

$$L = \frac{\lambda}{n - \sin(\theta)} \qquad (1)$$

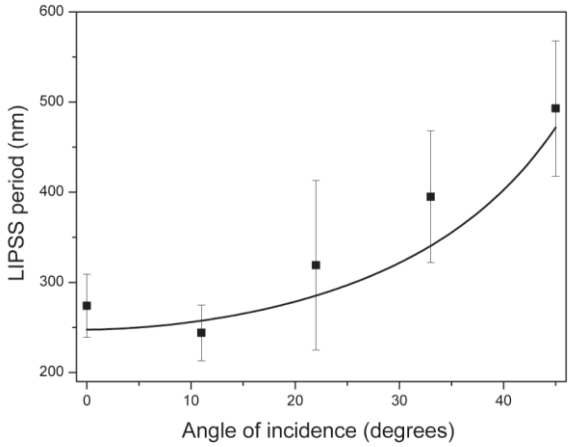

FIGURE 3. Variation of the LIPSS period with the laser incidence angle on a PET thin film sample. Irradiation was performed at 266 nm applying 1200 pulses of 6 ns with a fluence of 7 mJ/cm^2. The continuous line is the result of the fit to eq. (1).

The morphology of the structures can also be modified by control of laser polarization. In the experiment, the laser polarization was tuned from linear to circular using a rotating quarter wavelength plate positioned in front of the sample. The initial periodic linear structures resulted in circular bumps, as shown in Figure 4 for a PET thin film. In this case, irradiation with 1200 pulses of 266 nm and 6 ns with fluence of 7 mJ/cm^2 resulted in structures of ca. 400 nm diameter.

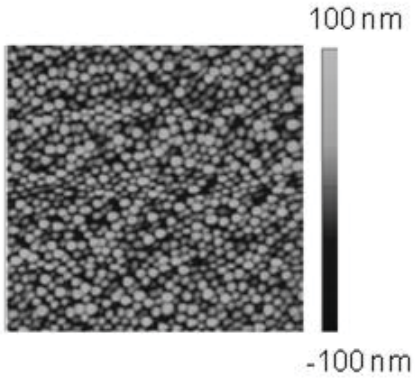

FIGURE 4. AFM image (5x5 μm^2 size) of structures created by irradiating a PET thin film with 1200 laser pulses of 6 ns and 7 mJ/cm^2 using circularly polarized light at the wavelength of 266 nm.

APPLICATION FOR SERS

To check if the initial rippled topography of the thin film polymer surface was maintained after PLD gold coating, the samples were analyzed by AFM. It was found that the periodic structure retained the initial relief and period. To investigate the applicability of the gold coated samples as SERS substrates, the compound thiophenol was used as a model analyte. Drops of aqueous solutions of thiophenol in different concentrations were poured onto gold coated unrippled and rippled polymer substrates and Raman spectra were acquired and compared. Additionally, for further comparison, control experiments were performed on an uncoated silicon substrate. Figure 5 shows the Raman spectra of thiophenol (at a concentration of 98 %) on silicon and of the same analyte at a concentration of 10^{-3} M on gold coated unstructured and LIPSS structured PTT samples. While the Raman signal from thiophenol is absent in the spectrum obtained from the silicon substrate, bands at 1002, 1020, and 1070 cm^{-1}, assigned to the molecular ring, are clearly visible on the gold coated substrates. An intensity enhancement of thiophenol bands by a factor of about 10-15 is observed in the spectra acquired on the nanostructured gold coated PTT substrate suggesting that the devised approach is effective for the preparation of active SERS substrates. Work is in progress to further enhance the SERS response of the gold coated LIPSS substrates.

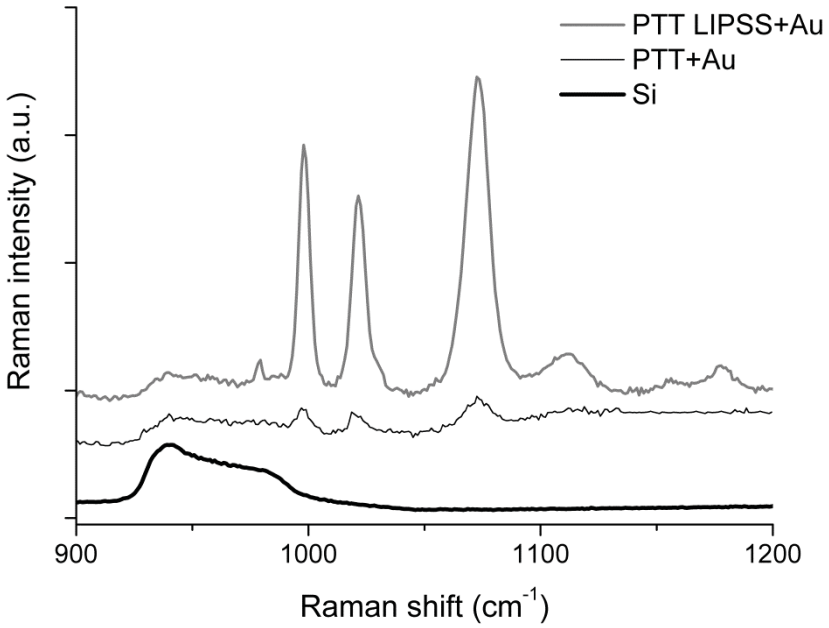

FIGURE 5. Raman spectra of 10^{-3} M thiophenol in aqueous solution on a silicon substrate and on the surfaces of gold coated PTT (PTT+Au) and gold coated nanostructured PTT (PTT+LIPSS+Au). LIPSS were fabricated at 266 nm with 600 pulses of 6 ns with a fluence of 7 mJ/cm^2. The spectra were recorded at the excitation wavelength of 785 nm.

CONCLUSIONS

In conclusion, laser irradiation of thin films of synthetic polymers and biopolymers results in the formation of LIPSS using linearly polarized light at fluences well below the ablation threshold in a wide range of laser pulse durations ranging from ns to fs. While production of LIPSS with ns pulses is only possible at highly absorbed UV wavelengths, irradiation with fs pulses results in ripple formation both in the UV and IR wavelengths, due to the efficient coupling of laser photons to the substrate mediated by multiphoton absorption. In all cases studied, the period of the structures is around the wavelength of the irradiation laser. The ripple period can also be modified by changing the angle of incidence of the laser beam on the substrate and the morphology of the superficial structures can be tuned to circular bumps by using circularly polarized laser. The presented strategies illustrate the possibility of control of the nanostructures created in polymer films in order to match the requirements derived from specific applications. As an example, it has been shown that gold coated rippled polymer films serve as SERS substrates enhancing the Raman signal of the model analyte thiophenol.

ACKNOWLEDGMENTS

This research is funded by MICINN, Spain, Projects CTQ2010-15680 and MAT2009-07789. E.R. and S.P. thank MICINN, Spain, for a Juan de la Cierva contract and an FPI fellowship respectively. Collaborations with the groups of C. Domingo (Instituto de Estructura de la Materia, CSIC, Madrid, Spain) and of P. Moreno (Universidad de Salamanca, Spain) are thankfully acknowledged.

REFERENCES

1. J.G. Fernandez, C.A. Mills, J. Samitier, *Small* **5***,* 614 (2009).
2. A. Ranella, M. Barberoglou, S. Bakogianni, C. Fotakis and E. Stratakis, *Acta Biomaterialia* **6**, 2711 (2010).
3. E. Rebollar, G. Bounos, M. Oujja, S. Georgiou, M. Castillejo, *J. Phys. Chem. B* **110**, 16452 (2006).
4. S. Gaspard, M. Oujja, R. de Nalda, M. Castillejo, L. Bañares, S. Lazare and R. Bonneau, *Appl. Phys. A,* **93**, 209 (2008).
5. S. Gaspard, M. Forster, C. Huber, C. Zafiu, G. Trettenhahn, W. Kautek, M. Castillejo, *Phys. Chem. Chem. Phys.* **10**, 6174 (2008).
6. E. Rebollar, S. Pérez, J.J. Hernández, I. Martín-Fabiani, D.R. Rueda, T.A. Ezquerra, M. Castillejo, *Langmuir* **27,** 5596 (2011).
7. E. Rebollar, J.R. Vázquez de Aldana, J.A. Pérez-Hernández, T.A. Ezquerra, P. Moreno, M. Castillejo, *Appl. Phys. Lett.* **100**, 041106 (2012).
8. M. Oujja, S. Pérez, E. Fadeeva, J. Koch, B.N. Chichkov, M. Castillejo, *Appl. Phys. Lett.* **95,** 263703 (2009).
9. R. Seemann, E.J. Kramer, F.F. Lange, *New Journal of Physics* **6**, 111 (2004).
10. M. Castillejo, E. Rebollar, M. Oujja, M. Sanz, A. Selimis, A. Sigletou, S. Psycharakis, A. Ranella, C. Fotakis, *Appl. Surf. Sci.* DOI: 10.1016/j.apsusc.2012.05.118.
11. K. Busch, G. von Freymann, S. Linden, S.F. Mingaleev, L. Tkeshelashvili, M. Wegener, *Physics Reports* **444**, 101 (2007).
12. M. Bolle, S. Lazare, M.Le Blanc, A.Wilmes, *Appl. Phys. Lett.* **60**, 674 (1992).
13. M. Csete, S. Hild, A. Plett, P. Zlemann, Zs. Bor, O. Marti, *Thin Solid Films* **453,** 114 (2004).
14. M. Forster, W. Kautek, N. Faure, E. Audouard, and R. Stoian, *Phys. Chem. Chem. Phys.* **13**, 4155 (2011).
15. S. Baudach, J. Bonse, and W. Kautek, Appl. Phys. A **69**, S395 (1999).
16. D. Bäuerle, *Laser Processing and Chemistry*, Berlin Springer-Verlag, 2000.
17. J.J. Hernández, D.R. Rueda, M.C García-Gutiérrez, A. Nogales, T.A. Ezquerra, M. Soccio, N. Lotti, A. Munari, *Langmuir* **26**, 10731 (2010).
18. P. Müller-Buschbaum, *A basic introduction to Grazing Incidence Small-Angle X-Ray Scattering,* in *Lectures Notes in Physics.* Berlin Springer-Verlag **776**, 61-89 (2009).
19. M. Walczak, M. Oujja, J.F. Marco, M. Sanz, M. Castillejo, *Appl. Phys. A* **93**, 735 (2008).